Local SAR reduction in multi-slice pTx via "SAR hopping" between excitations

Bastien Guerin[1], Elar Adalsteinsson[2,3], and Lawrence L. Wald[1,3]

[1]Martinos Center for Biomedical Imaging, Dept. of Radiology, Massachusetts General Hospital, Charlestown, MA, United States, [2]Dept of Electrical Engineering and Computer Science, Massachusetts Institute of Technology, Cambridge, MA, United States, [3]Harvard-MIT Division of Health Sciences Technology, Cambridge, MA, United States

Introduction: SAR induced temperature increases are difficult to measure [1] or calculate [2]. Therefore SAR, in addition to temperature, is regulated [3]. Since the time scale of temperature changes (~1min.) is long compared to a single RF pulse, only SAR averaged over several pulses is relevant to tissue temperature, not the SAR of individual pulses. In [4]-[6] the authors proposed exciting different k-space lines within a single slice using different pulse waveforms with different 10g SAR distributions in order to reduce the pulse-averaged local SAR at constant excitation error. This strategy will result in ghosting if significant flip angle or excitation phase variations exist between the different pulses. In this work, we propose a similar local SAR averaging strategy where different slices utilize different pulses which are jointly optimized so as to minimize their peak average SAR. Since all k-space lines in a given slice are excited by a single pulse, ghosting is not an issue. Moreover, differences between the B1+ profiles of the transmit channels at different z positions increase the variability between pulses, making it easier to design pulses with uniform excitations at each slice but different spatial SAR distributions.

Methods: We simulated a pTx body array with 16 channels distributed in two rows of eight loops modeled independently (no coupling) using the FDTD software SEMCAD (SPEAG, Zurich) and the 77 tissue classes, 1mm resolution Virtual Family phantom "Duke" (IT'IS Foundation, Zurich) [7]. Complex B1+ maps and SAR matrices were extracted from the $\mathbf{H}$ and $\mathbf{E}$ fields created by each loop. The 338,101 SAR matrices corresponding to every voxel of the body model were compressed to 3,868 Virtual Observation Points (VOPs) allowing fast monitoring of local SAR in the whole body with a SAR overestimation less than 1% [8]. RF shimming and 2-spoke excitation pulses were designed attempting to create a uniform 10° flip angle distribution at transverse slices z=±9cm by solving (joint design): $\min_{\mathbf{x}} \|\mathbf{A}\mathbf{x}-\mathbf{b}\|_2^2$ s.t. *a)* $\sum_{k=1}^{K}\mathbf{x}_k\mathbf{S}_n\mathbf{x}_k^H \le KS_{\max}^{local}\ \forall n$; *b)* $\sum_{k=1}^{K}\mathbf{x}_k\langle\mathbf{S}\rangle\mathbf{x}_k^H \le KS_{\max}^{global}$; *c)* $\|\mathbf{x}\|_\infty^2/50 \le P_{\max}$, where $\mathbf{A}$ is the many-pulses gradient matrix, $\mathbf{x}$ is the vector of spoke amplitudes, $\mathbf{b}$ is the complex target magnetization, K is the number of pulses (equal to the number of slices), $\mathbf{S}_n$ are the local SAR matrices (VOPs), $\langle\mathbf{S}\rangle$ is the global SAR matrix, and $S_{\max}^{local}$, $S_{\max}^{global}$ and $P_{\max}$ are the maximum local and global SAR and max. forward power. This optimization problem is a joint design of all slice excitations, i.e. $\mathbf{A}$ is a bloc-diagonal matrix made of the gradient matrices of each pulse k and $\mathbf{x}$ is the concatenation of spoke amplitudes for each pulse $\mathbf{x}_k$, constraining the pulse-averaged local SAR. RF shimming and 2 spokes pulses were also designed while constraining the local SAR of each pulse independently (independent design). L-curves quantifying the tradeoff between local SAR versus excitation error were obtained by varying the local SAR constraint (global SAR and max. forward power constraints were set to 5W/kg and 50kW total forward power).

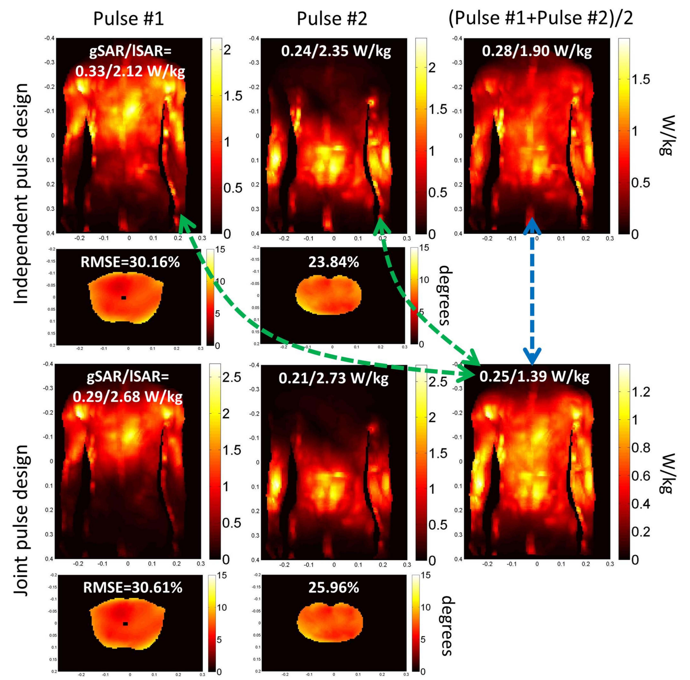

Fig. 1. SAR and flip angle maps corresponding to pulses #1 and #2 (and their average) designed independently (local SAR constraints for each pulse) and jointly (local SAR constraints for the average of pulses). ***Green dash arrows:*** *Joint multislice >> independent single slice.* ***Blue dash arrow:*** *Joint multislice > independent multislice.*

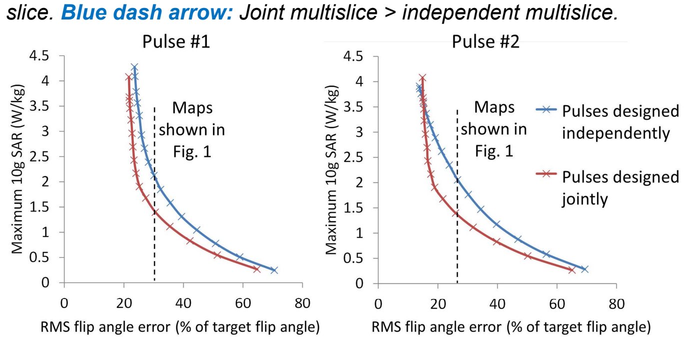

Fig. 2. L-curves quantifying the tradeoff between local SAR and excitation error for the independent and joint multislice pulse designs.

Results: Fig. 1 shows SAR and flip angle maps associated to the two RF shimming slice excitations designed jointly and independently with similar excitation errors. Although each pulse of the joint design had a peak local SAR greater than that of the pulses designed independently, the peak pulse-averaged local SAR was lower because their SAR distributions overlapped minimally. We found that jointly designing the two z-pulses yielded a lower pulse-averaged local SAR at constant excitation error than when designing them independently: local SAR was reduced by 50-70% (30-35%) with the joint/multislice approach compared to the independent/single slice (independent/multislice) approach. Fig. 2 shows that this effect is robust at all SAR/exc. error levels. Reduction of pulse-averaged local SAR was possible because the two slices utilized different rows of the array. For 2 spokes excitations, this improvement was much less pronounced because spokes pulses always utilized heavily both rows (the row further from the imaging slice has a different spatial profile that is used by multiple spokes pulses to improve fidelity). This indicates that application of this multislice technique in multiple spokes excitations and/or single row pTx arrays will require, in addition to the joint pulse design proposed here, an automatic design of gradient trajectories yielding pulses with good excitation properties and minimally overlapping SAR distributions.

References:

[1] Shapiro, E. M. (2002). MRM **47**(3): 492-498.
[2] Yeung, C. J. (2001). Med. Phys. **28**: 826.
[3] Shellock, F. G. (1991). JMRI **1**(1): 97-101.
[4] Homann, H., (2010). MRM **65**(2): 350-357.
[5] Graesslin, I. (2009). Proc. ISMRM **58**(2).
[6] Zelinski, A. (2008). Res. Lab. of Elect., MIT. **Ph. D.**
[7] Christ, A. (2010). Phys. Med. Biol. **55**: N23.
[8] Eichfelder, G. (2011). MRM **66**(5): 1468-1476.